J|A|C|S
JOURNAL OF THE AMERICAN CHEMICAL SOCIETY
ARTICLE
pubs.acs.org/JACS

Extended Two-Dimensional Metal−Organic Frameworks Based on Thiolate−Copper Coordination Bonds

Hermann Walch,[†] Jürgen Dienstmaier,[†] Georg Eder,[†] Rico Gutzler,[†,#] Stefan Schlögl,[†] Thomas Sirtl,[⊥] Kalpataru Das,[‡] Michael Schmittel,[‡] and Markus Lackinger[*,†,§,⊥]

[†]Department for Earth and Environmental Sciences and Center for NanoScience, Ludwig-Maximilians-Universität, Theresienstrasse 41, 80333 München, Germany

[‡]Center of Micro and Nanochemistry and Engineering, Organische Chemie I, Universität Siegen, Adolf-Reichwein-Strasse 2, 57068 Siegen, Germany

[§]Deutsches Museum, Museumsinsel 1, 80538 München, Germany

[⊥]Technical University Munich, TUM School of Education, Schellingstrasse 33, 80799 München, Germany

S *Supporting Information*

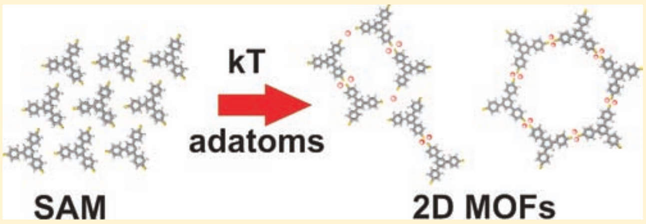

ABSTRACT: Self-assembly and surface-mediated reactions of 1,3,5-tris(4-mercaptophenyl)benzene—a three-fold symmetric aromatic trithiol—are studied on Cu(111) by means of scanning tunneling microscopy (STM) under ultrahigh-vacuum (UHV) conditions. In order to reveal the nature of intermolecular bonds and to understand the specific role of the substrate for their formation, these studies were extended to Ag(111). Room-temperature deposition onto either substrate yields densely packed trigonal structures with similar appearance and lattice parameters. Yet, thermal annealing reveals distinct differences between both substrates: on Cu(111) moderate annealing temperatures (∼150 °C) already drive the emergence of two different porous networks, whereas on Ag(111) higher annealing temperatures (up to ∼300 °C) were required to induce structural changes. In the latter case only disordered structures with characteristic dimers were observed. These differences are rationalized by the contribution of the adatom gas on Cu(111) to the formation of metal-coordination bonds. Density functional theory (DFT) methods were applied to identify intermolecular bonds in both cases by means of their bond distances and geometries.

INTRODUCTION

In the past years a great structural and chemical variety of surface-supported metal−organic networks has been demonstrated by combining appropriately functionalized organic building blocks with various coordinating metals.[1] While some of the coordination complexes utilized for surface-confined systems were already well-known from bulk systems, other coordination numbers and geometries are unique to surface-supported networks. Concerning the intermolecular bond strength, and thus the overall stability of the structures, metal−organic networks occupy an intermediate position between hydrogen-bonded networks and covalent organic frameworks.[1a] Yet, since metal-coordination bonds are reversible under commonly applied growth conditions, the preparation of long-range ordered networks becomes feasible. The motivation of this work is to extend the tool box of functional groups for the design of surface-supported metal−organic networks to thiol groups and understand the formation kinetics and topological properties of thiolate−metal complexes. To this end we designed and synthesized a highly symmetric aromatic trithiol molecule and studied its self-assembly and surface-supported reactions by means of scanning tunneling microscopy on a Cu(111) surface, which is known to inherently supply copper coordination centers from its free adatom gas.[2] To clarify the specific role of the substrate, similar experiments were also conducted on Ag(111). Thiolate−copper coordination bonds are of particular interest because of their electronic conjugation which allows electronically coupling of molecular units by thiolate−copper−thiolate bonds.[3] One conceivable application of copper−thiolate complexes hence lies in the field of molecular electronics, where reliable tools are required for interconnection of molecular entities in an atomically defined manner without perturbing or interrupting electronic conjugation.

EXPERIMENTAL DETAILS

All samples were prepared and characterized in an ultrahigh-vacuum chamber (base pressure $<5 \times 10^{-10}$ mbar) equipped with an Omicron VT scanning tunneling microscope (STM). Cu(111) single crystals were prepared by subsequent cycles of Ar$^+$-ion sputtering and annealing at 820 K. Additional low energy electron diffraction (LEED) experiments for further characterization of the precursor structure were carried out in a separate UHV system equipped with standard preparation facilities and LEED optics from Omicron. LEED measurements were

Received: February 8, 2011
Published: May 02, 2011

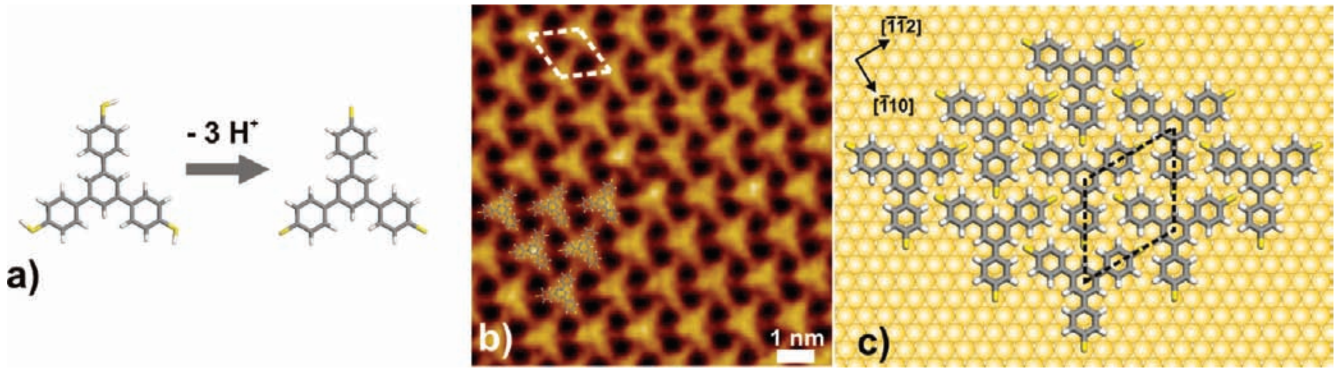

Figure 1. (a) TMB fully deprotonates upon room temperature adsorption on reactive copper surfaces forming a surface-anchored trithiolate. (b) STM topograph of as-deposited TMB on Cu(111) acquired at room temperature (I_T = 185 pA, U_T = 0.79 V, 10 × 10 nm^2, $a = b$ = 1.30 nm, γ = 120°, unit cell indicated by dashed white lines). The densely packed trigonal structure contains one molecule per unit cell. (c) Tentative model of the densely packed trithiolate structure including the Cu(111) substrate. While the azimuthal orientation of the TMB-derived trithiolates with respect to the substrate directions can be inferred from the experiment, the precise adsorption site is not known.

carried out at a sample temperature of ~50 K maintained by a closed-cycle helium cryostat. 1,3,5-Tris(4-mercaptophenyl)benzene (TMB) was thermally evaporated from a home-built Knudsen cell with crucible temperatures around 145 °C. During deposition and STM imaging the substrate was held at room temperature. STM images were acquired at room temperature and processed by line-wise leveling and 3 × 3 Gaussian filtering.

■ RESULTS AND DISCUSSION

In this work, adatom-mediated coordination of TMB (cf. Figure 1a) on Cu(111) into two-dimensional (2D) metal–organic networks based on thiolate–copper coordination bonds is presented. Bulk synthesis already yielded copper–thiolate metal–organic frameworks (MOF)[3] and linear polymeric structures.[4] While surface-confined coordination networks based on copper–carboxylate coordination bonds have been reported by several groups,[1d,2b,5] to our knowledge, this type of interlinking chemistry has not been utilized for surface-supported 2D systems. We demonstrate that upon thermal annealing an initial precursor structure is converted into copper–thiolate coordinated networks mediated by the free-adatom gas of the Cu(111) surface. Interestingly, the thiolate–copper complexes found in this study contain copper dimers which coordinate two thiolates. In bulk MOFs, interconnects typically consist of single metal atoms as coordination centers. In the proposed system the coordinating metal dimers are additionally stabilized by adsorption on the surface, possibly rendering them unique for surface-confined systems.

In a first preparation step TMB is deposited by thermal sublimation under ultrahigh-vacuum (UHV) conditions on Cu(111) at room temperature and characterized by means of *in situ* STM and LEED. Figure 1b depicts an STM topograph of the resulting self-assembled densely packed trigonal structure with an STM-derived lattice parameter of (1.30 ± 0.05) nm. Accompanying LEED measurements (cf. Supporting Information) aid to identify the monolayer as a commensurate $3\sqrt{3} \times 3\sqrt{3}$ R30° superstructure. Upon adsorption on reactive metal surfaces thiols deprotonate and become thiolates which are anchored by sulfur–metal bonds.[6] Both the size of the unit cell and the three-fold symmetric appearance of adsorbed TMB in STM topographs substantiate the assumption that TMB fully deprotonates on Cu(111) and forms three covalent S–Cu bonds with the substrate; a tentative model of the precursor structure is depicted in Figure 1c. However, the formation of a densely packed monolayer indicates a non-negligible contribution from intermolecular interactions for structure formation. While the azimuthal orientation of TMB within the unit cell and with respect to the substrate can be inferred from STM topographs, its absolute adsorption position with respect to the copper substrate remains unknown. Interestingly, the TMB-derived trithiolate molecule is also commensurate with the substrate; i.e. for its actual azimuthal orientation all sulfur atoms reside on similar adsorption sites and can thus simultaneously optimize their interaction with the substrate. Covalent anchoring by three peripheral sulfur groups stabilizes a planar adsorption geometry of TMB on Cu(111), whereas monothiolates tend to adsorb upright,[6d,7] or inclined, as it is the case for halogen-substituted thiophenols.[8]

In a second preparation step, thermal annealing at 160–200 °C for ~10 min converts the self-assembled trithiolate monolayers into two polymorphs which are both identified as metal–organic coordination networks. STM topographs of both metal-coordinated polymorphs are depicted in Figure 2. Conversion of the initial precursor structure into 2D metal-coordinated networks is accompanied by substantial reorientation and repositioning of TMB molecules, but most importantly by introducing intermolecular copper–thiolate coordination bonds.

The effect of annealing is 2-fold: First lateral mobility of the trithiolate species is enhanced. Second, the area density of the free copper adatom gas is greatly increased, whereby a sufficient amount of highly mobile coordination centers is supplied.

The influence of a 2D adatom gas has been recognized as an important contribution to the surface chemistry of metals.[9] The adatom gas originates from a temperature-dependent evaporation/condensation equilibrium at step-edges. At lower temperatures, processes with lower activation energies are dominant, i.e. mass transport along step-edges. For higher temperatures mass exchange between step-edges and terraces is the dominant process[10] leading to a drastic increase of the free adatom concentration already at moderate temperatures of ~500 K.[11] Conversion of initially intermolecular hydrogen-bonded networks into metal–organic networks on Cu(111) in this temperature range have similarly been reported by Matena[2b]

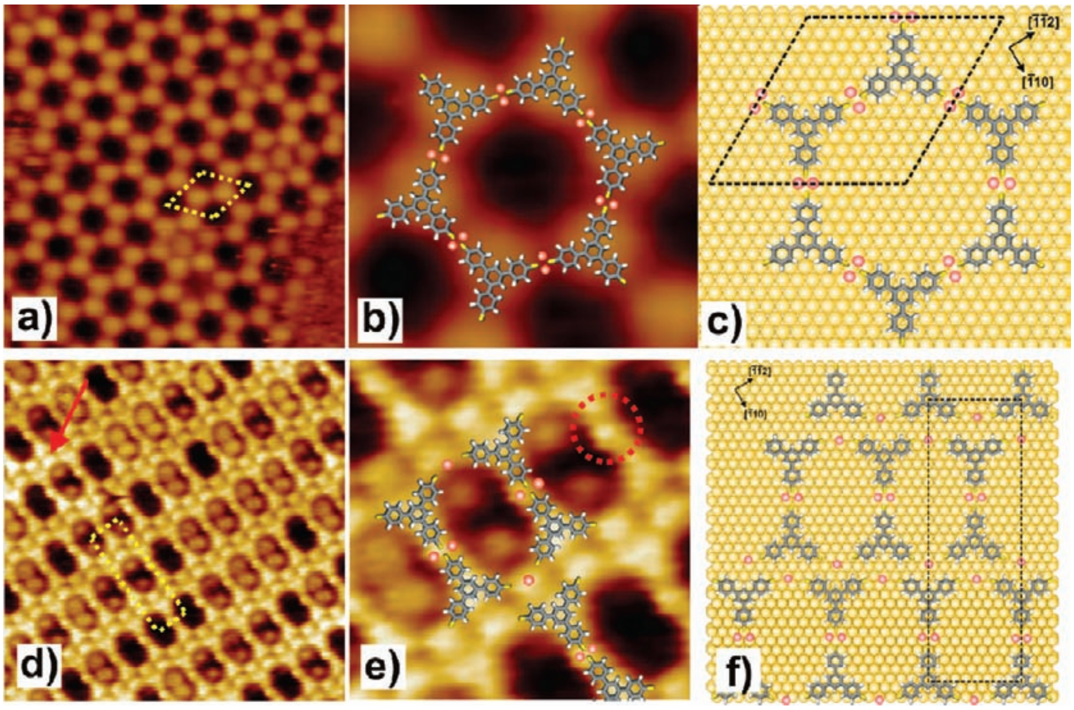

Figure 2. (a) STM topograph of honeycomb structure with unit cell indicated ($U_T = -1.0$ V, $I_T = 67$ pA, 24 × 24 nm^2, $a = b = 3.4$ nm, $\gamma = 120°$) and (b) close-up (6.5 × 6.5 nm^2) of honeycomb structure with molecular model. (c) Tentative model of the honeycomb structure including the substrate; the hexagonal unit cell is indicated by black dashed lines. (d) STM topograph of dimer row structure with unit cell indicated ($U_T = -0.8$ V, $I_T = 121$ pA, 18 × 18 nm^2, $a = 2.2$ nm, $b = 6.6$ nm, $\gamma = 90°$) and (e) close-up (6.9 nm × 6.9 nm^2) of dimer row structure with molecular model. Protruding features are observed in the STM contrast at the center of a dimer (marked by the dashed circle) and hint toward metal coordination. (f) Tentative model of the dimer row structure including the substrate; the rectangular unit cell is indicated by black dashed lines.

and Pawin.[2a] In the latter work, annealing at lower temperatures leads to a partially hydrogen-bonded and partially metal-coordinated polymorph. As already mentioned above for TMB, two different metal-coordinated networks, a hexagonal honeycomb and a centered rectangular dimer row structure emerge. In both structures copper adatoms coordinate TMB molecules via their thiolate groups.

The hexagonal honeycomb structure (Figure 2a−c) has a lattice parameter of 3.4 nm and belongs to the plane space group *p6mm*. The second structure is less symmetric (*c2mm*) and is composed of rows of dumbbell-shaped dimers (Figure 2e−f). Adjacent dimer rows are offset by exactly half a lattice parameter exactly along the row axes, resulting in a rectangular centered nonprimitive unit cell. During the conversion of the densely packed precursor structure into the porous networks, entrapment of excess TMB molecules within the pores occurs frequently and gives rise to additional contrast features within the pores as evident from Figure 2. This observation is in accord with other experiments on periodic and irregular porous surface-supported networks where molecules, either deposited in excess, captured during structure formation,[12,13] or additionally deposited[14], were likewise trapped within the pores.

The honeycomb and dimer row structure were observed in coexistence as shown in Figure 3. The relative ratio of both phases slightly depends on the initial coverage of the precursor structure, with a preference for the more densely packed dimer row structure at higher coverages. It is noteworthy that the morphology of the two metal-coordinated TMB polymorphs resembles those of rubrene monolayers both on (110) and (111) copper surfaces[15] and Au(111).[16] Yet, despite the similar appearance of rubrene vs TMB monolayers in STM topographs, their self-assembly is notably different. In the gas phase rubrene is highly nonplanar and even remains nonplanar after adsorption. TMB, on the other hand, is slightly nonplanar in the gas phase due to an out-of-plane rotation of its peripheral mercaptophenyl units with respect to the phenyl ring at the center. However, the

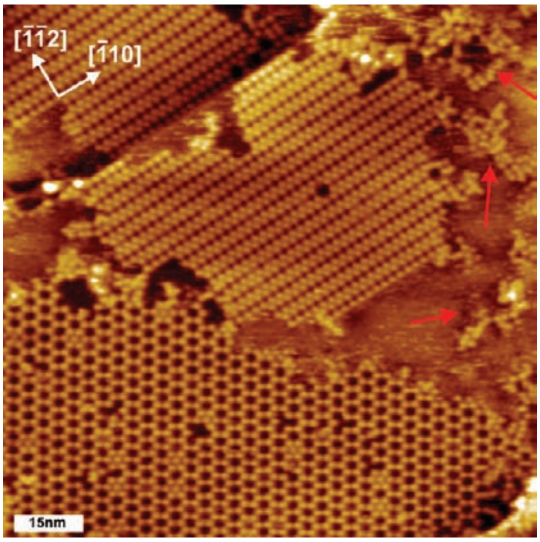

Figure 3. Overview STM topograph illustrating the coexistence of both phases ($U_T = -1.64$ V, $I_T = 66$ pA, 116 × 116 nm^2) on Cu(111). Red arrows indicate first occurrence of degraded molecules starting to appear at annealing temperatures around 220 °C. White arrows indicate crystallographic directions of the substrate.

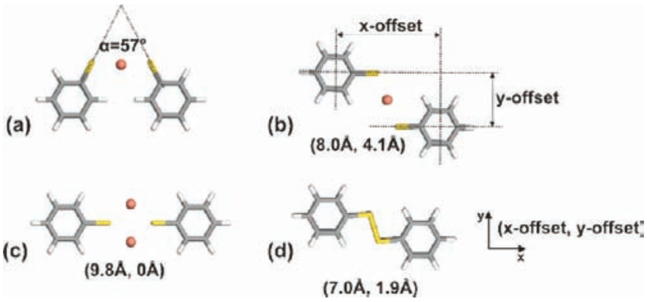

Figure 4. DFT geometry optimized intermolecular bonding schemes for interconnected phenylthiolates via (a) one-center *trans*-coordination *syn*-conformation (α = 57°), (b) one-center *trans*-coordination *anti*-conformation (*x*-offset = 8.0 Å, *y*-offset = 4.1 Å), (c) two-center coordination bond (*x*-offset = 9.8 Å, no *y*-offset), (d) covalent coupling via disulfur-bridge (*x*-offset = 7.0 Å, *y*-offset = 1.9 Å). For all bonds, the center-to-center distance of the phenyl groups (*x*-offset) and the perpendicular axial offset (*y*-offset) respectively are given in parentheses.

mirror symmetric STM appearance of TMB in all observed structures suggests that it becomes planar upon adsorption due to interactions with the substrate. Also the pronounced chirality of rubrene affects its self-assembly and leads to the expression of chiral structures and aggregates,[17] while no indication of chirality is discernible in any of the TMB structures. Lastly, the interactions which drive self-assembly are distinctly different for rubrene and TMB. In the precursor structure of TMB, covalent bonds between sulfur and copper play an important role, whereas after the phase transition metal coordination becomes the predominant interaction. On the other hand, these types of interactions are absent in rubrene self-assembly, where van der Waals interactions, higher multipole electrostatic interactions, and substrate-mediated interactions govern structure formation.[18]

For a fundamental understanding of the thiolate—copper coordination bonds, DFT calculations (cf. Supporting Information for details) have been performed of the connecting nodes, modeled by two phenylthiolates and corresponding copper centers. Four different intermolecular bonding schemes were considered: metal-coordination bonds mediated by one or two copper atoms, and a covalent disulfur bridge. Motivated by experimental results on thiolate—gold complexes[19] both *syn*—*trans* and *anti*—*trans* arrangements were taken into account for the one-center coordination bonds. To reduce the computational cost only the outer phenylthiolate parts were simulated, and for ease of calculations the explicit substrate influence has been neglected in this first approximation. Typically, intermolecular bond lengths of adsorbed systems are altered in comparison to the gas phase, but these differences are normally small and, especially for large entities, often below the accuracy of STM measurements. DFT results on these simplified model systems are depicted in Figure 4. Major findings can be summarized as follows. Only two-center coordination bonds facilitate linear interconnection. One-center coordination bonds and covalent disulfur bridges both result in lateral offsets perpendicular to the bond axis.

The one-center *anti* conformational arrangement and the disulfur bridge result in a lateral bond offset of ~4.1 Å and ~1.9 Å, respectively. These lateral offsets are sufficiently large to be identifiable in STM topographs. In the one-center *syn* conformational assembly the molecular axes include an angle of 57°, which is significantly larger than the 35° reported for Au-coordinated methylthiolate by Voznyy and co-workers.[19] This can readily be explained by steric repulsion, being more pronounced for the bulky phenyl ligands as compared to that for methyl groups.

According to DFT results, the total binding energy of two-center coordination complexes is strongest with a value of 555 kJ/mol. Total binding energies of *trans*—*syn* (394 kJ/mol) and *trans*—*anti* (397 kJ/mol) one-center coordination complexes are comparable, but notably lower than for the two-center complex. The covalent disulfur bridge is the weakest bond with a strength of 151 kJ/mol. Covalent S—S bonds exhibit a certain variability of bond angles and energies,[20] with the latter value being within the typical range.

Both the honeycomb and the dimer row structure contain dumbbell shaped TMB dimers as basic structural motif. High resolution STM images of both polymorphs occasionally show protruding features between dimers; an example is marked in Figure 2e. An additional STM topograph of the honeycomb structure very clearly showing protruding contrast features at the center position between adjacent molecules is provided in the Supporting Information (cf. Figure S2). Although these contrast features hint toward intermolecular bonds through metal-coordination, they do not allow to unambiguously infer the exact number of metal-coordination centers per bond. Yet, since no lateral displacement occurs along the dimer axis, the DFT calculations suggest coordination of the thiolate groups by two copper atoms as depicted in Figure 4c. This conclusion is further substantiated by comparison of experimental and theoretical bond lengths. STM data yield a center-to-center distance of 2.0 (±0.2) nm between two TMB molecules in the dimer. DFT results in combination with the intramolecular distance between central and outer phenyl rings in TMB (0.46 nm for a geometry optimized isolated molecule) postulate a dimer center-to-center distance of 1.90 nm. Accordingly, the experimental lattice parameter of the honeycomb structure (3.4 nm) is in good agreement with the anticipated lattice parameter from the two-center coordination interconnect (3.3 nm), while both the one-center coordination scenario (2.9 nm) and the covalent disulfur bridge (2.8 nm) would yield notably smaller lattice parameters. From the *p6mm* symmetry it can be concluded that all intermolecular bonds in the honeycomb structure are equivalent. A complete model of the honeycomb structure is overlaid in the STM topograph depicted in Figure 2b, and a tentative structural model including the substrate is separately presented in Figure 2c.

Yet, due to its lower symmetry the dimer row structure cannot consistently be explained solely on the basis of two-center coordination bonds. Thus, a bonding scheme is proposed involving different types of intermolecular bonds. Both appearance and center-to-center distance of dimers (~2.0 nm) within the rows are similar to the honeycomb structure. Also in both structures the dimers have the same orientation with respect to the Cu(111) substrate, i.e. their axes are oriented along the $\langle \bar{1}12 \rangle$ direction. This registry points toward a distinct epitaxial relation between the dimers and the Cu(111) substrate. Hence, it is concluded that also the dimers within the dimer row structure are similarly interconnected by two-center coordination bonds. These dimers assemble in parallel rows, where adjacent rows are shifted half a lattice parameter with respect to the row direction. STM topographs exhibit protruding contrast features directly above and below intrarow neighbors (marked in Figure 2d by a red arrow) which point toward a *trans*—*syn* arrangement, as implemented in the models in e and f of Figure 2, where the former is overlaid to the STM image and the latter model includes the substrate. Since coordinating copper atoms cannot be resolved separately, as is also the case for the two atoms coordinating the dimers, dimer−dimer coordination by more than one Cu atom cannot be excluded. Polynuclear copper−thiolate coordination bonds are common,[21] where coordinating copper clusters are further stabilized by cuprophilicity.[22] For instance, coordination by Cu_3 clusters has also been observed previously for bulk systems.[3]

Since the doubly copper-coordinated dimer is the structural motif of both the honeycomb and the dimer row structure, its adsorption geometry on the Cu(111) substrate is of particular interest. A tentative model which takes both the STM-derived orientation with respect to the substrate and the DFT-derived atomic configuration of the interconnect into account is provided in Figure 5. This model illustrates that both coordinating copper atoms could indeed adsorb at similar sites, for instance as tentatively shown in three-fold hollow sites. The actual distances between the two coordinating copper atoms in the proposed surface-confined metal-coordination complexes range most likely between the two extreme values, i.e. 2.87 Å as derived from our DFT calculations for a fully neglected and 2.55 Å—the Cu(111) lattice parameter—for a fully effective substrate influence. Therefore, in summary the actual Cu−Cu distance might result from a compromise and interplay between the periodic potential of the substrate which favors the smaller Cu−Cu spacing closer to the lattice constant and the gas phase Cu−Cu spacing which is more influenced by the orbital configuration and hybridization of the thiolate and the copper centers.

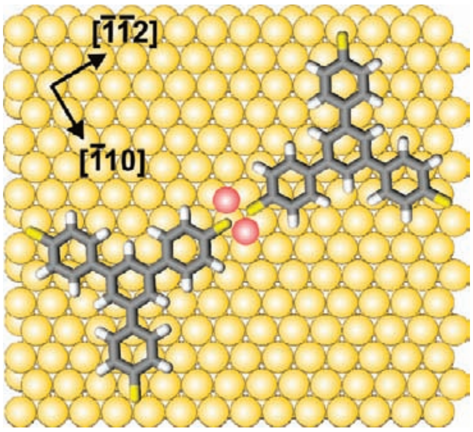

Figure 5. Tentative model of the adsorption geometry of a doubly copper coordinated TMB dimer including the Cu(111) substrate. Both coordinating copper atoms (colored red) could adsorb on similar lattice sites to simultaneously optimize their adsorption energy, e.g. as shown on three-fold hollow sites (yellow: substrate atoms).

In order to reveal the specific role of the Cu(111) substrate for the phase transition and to shed light on the chemical properties and reactivity of copper adatoms, the same type of experiments with similar sample preparation protocols were conducted on Ag(111). Room-temperature deposition of TMB on Ag(111) also yields a densely packed trigonal structure (cf. Figure 6a, $a = 1.35 \pm 0.05$ nm,). Since the lattice parameter of the trigonal structure on Ag(111) is similar to the value obtained on Cu(111) within experimental error, the precursor structure on Ag(111) is also identified as densely packed deprotonated trithiolates which are covalently anchored to the substrate through three peripheral thiolate−metal bonds. While the initial TMB precursor structures appear similar on both substrates, the response to thermal annealing is distinctly different on Ag(111): annealing up to 250 °C for ∼1 h did not result in a phase transition; however, after the sample annealed at 300 °C for ∼1 h, disordered glassy networks were observed in coexistence with remnants of the precursor structure; a typical STM topograph is depicted in Figure 6b. Nonperiodic glassy organic networks have recently gained substantial interest. Particularly nice examples include metal-coordination networks of nonlinear, prochiral ditopic organic linkers with cobalt atoms[23] and hydrogen-bonded cytosine networks on Au(111).[13b,24] Further, structurally comparable irregular organic networks have also been observed, when halogenated precursor molecules were polymerized by surface-mediated reactions into covalent networks.[25] While the irregularity of the glassy metal-coordination and hydrogen-bonded networks arises from the low symmetry of the building blocks in combination with the energetic equivalence of various different basic intermolecular bond motifs, the degree of disorder typically

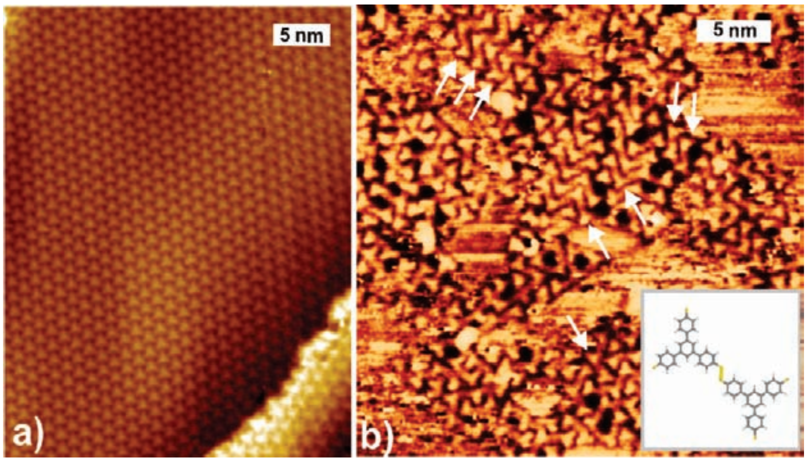

Figure 6. STM topographs of TMB deposited on Ag(111) (a) as-deposited at room temperature ($U_T = -0.33$ V, $I_T = 44$ pA, 30×39 nm^2) and (b) after annealing to 300 °C for ∼1 h ($U_T = -0.98$ V, $I_T = 85$ pA, 30×30 nm^2). The precursor structure on Ag(111) appears similar to Cu(111) with a similar lattice parameter of (1.35 ± 0.05) nm. Annealing of as-deposited samples at conditions which would already result in irreversible deterioration of the networks on Cu(111), yields a glassy disordered network on Ag(111). Within the disordered networks interconnected dimers can be discerned (marked by white arrows); their dimensions are consistent with formation of covalent disulfur bridges.

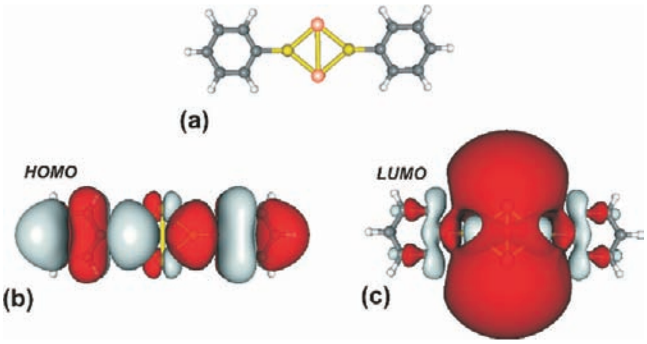

Figure 7. DFT results of structure and frontier molecular orbitals of a two-center coordination bond interconnecting two phenylthiolates (a) geometry, (b) HOMO, (c) LUMO of the complex.

observed for covalent networks is owed to the irreversibility of the covalent molecular interlinks under the growth conditions, which inhibits postcorrection of topological defects. A closer look at the disordered TMB structures on Ag(111) reveals dimers with a distinct lateral offset to the interconnecting axis; examples are marked in Figure 6b by white arrows. The lateral offset is consistent with DFT-derived values for disulfur bridges; consequently, we propose that the dimers observed after a thermal treatment of the precursor structure on Ag(111) are covalently interlinked.

An interesting, not entirely solved question is why adatom-mediated formation of metal-coordination networks was observed for the same TMB molecules on Cu(111) but not on Ag(111). On both substrates, the densely packed precursor structures obtained upon room temperature deposition are structurally quite similar, and differences in their precise epitaxial relations between both substrates can hardly account for the absence of metal-coordination networks on Ag(111). Also the temperature dependent densities of the adatom gases on both surfaces are comparable[26] ruling out adatom availability as a decisive criterion. Even more so, since tempering the Ag(111) samples up to significantly higher temperatures should have provided a sufficient amount of adatoms. Nevertheless, silver coordinated TMB metal−organic networks have never been observed, but only irregular networks. The absence of metal-coordination networks on Ag(111) is best explained by a different affinity of Cu vs Ag adatoms to form metal-coordination bonds with thiolates. This hypothesis is in accord with experimental findings on the adatom-mediated formation of carboxylate-based metal-coordination networks on Cu(111) vs Ag(111). While metal-coordination networks of trimesic acids were readily observed on Cu(111), their formation was again absent on Ag(111).[9] Interestingly, preceding deposition of copper onto Ag(111) promoted the formation of trimesic acid metal-coordination networks also on this substrate. These results are consistently explained by the assumption that copper deposition on Ag(111) introduces a copper adatom gas which is in equilibrium with the deposited copper islands. The higher reactivity of this artificially introduced, extrinsic copper adatom gas is the driving force for formation of copper metal-coordination networks.

Moreover, the present results on covalently interlinked TMB molecules on Ag(111) indicate that the lateral offset of disulfur-bridged molecules can clearly be resolved in STM and hence indirectly prove that the porous TMB networks on Cu(111) are not built up by disulfur-bridged molecules.

In order to illustrate the electronic properties of the copper−thiolate metal-coordination interlink, DFT derived frontier molecular orbitals are depicted in Figure 7. Evidently, both HOMO and LUMO of bicoordinated phenylthiolates exhibit intensity at the bond site. The LUMO appears to be more localized at the bond, whereas the HOMO is evenly distributed across the metal-coordination complex. Such delocalization allows for coherent electron transport through the metal-coordination bond, rendering this interconnection chemistry a suitable candidate for interlinking single molecules into more complex molecular electronics circuitry.

■ SUMMARY

In summary, adatom-mediated 2D metal−organic networks were synthesized on Cu(111) by thermal annealing of a self-assembled precursor structure. The two observed metal−organic networks are based on metal-coordination bonds between thiolates and either one or two copper adatoms. Comparison between DFT-derived and experimental bond lengths and geometries aided in the identification of intermolecular coordination bonds. In contrast, deposition on Ag(111) resulted in a similar precursor structure, but annealing at higher temperatures only resulted in irregular structures, where monomers are interconnected by covalent disulfur bridges. These pronounced differences between both surfaces are explained by a higher affinity of copper adatoms as compared to silver adatoms to form metal-coordination bonds with thiolates.

As suggested by the spatial distributions of their frontier molecular orbitals, copper−thiolate complexes are fully electronically conjugated. This intriguing feature renders copper−thiolate coordination bonds particularly interesting for organic conductors and molecular electronics. Especially the envisioned molecular electronics applications not only require precise electronic function within a single molecule but also equally directional communication between molecules. Yet, up to now the issue of interconnecting single-molecule devices into more complex circuits is not satisfactorily addressed. Numerous studies concluded that, for contacts and interconnects, bond topology on the atomic level is of utmost importance due to the coherent nature of electron transport in molecular electronics. Hence, means to interconnect molecular entities in an atomically defined manner without perturbing or interrupting electronic conjugation are urgently required. Thiol groups in combination with copper coordination centers are ideally suited as "solder" for molecular electronics due to their electronic conjugation, their relatively high stability, and not at least due to their compatibility with self-assembly bottom-up fabrication techniques.

■ ASSOCIATED CONTENT

Ⓢ Supporting Information. Synthesis and calculational details, additional LEED and STM results. This material is available free of charge via the Internet at http://pubs.acs.org.

■ AUTHOR INFORMATION

Corresponding Author

markus@lackinger.org

Present Address

[#]Institut National de la Recherche Scientifique, Université du Québec, 1650 boulevard Lionel-Boulet, Varennes, QC, J3X 1S2 Canada.

■ ACKNOWLEDGMENT

Financial support by the Deutsche Forschungsgemeinschaft (DFG) within the Nanosystems-Initiative Munich (NIM) and with FOR 516 (Siegen) is gratefully acknowledged. St.S. and G.E. are particularly grateful for support by the Elitenetzwerk Bayern and the Hanns-Seidel Stiftung. T.S. acknowledges support by the Fonds der Chemischen Industrie.

■ REFERENCES

(1) (a) Barth, J. V. *Annu. Rev. Phys. Chem.* **2007**, *58*, 375–407. (b) Stepanow, S.; Lin, N.; Barth, J. V. *J. Phys.: Condens. Matter* **2008**, *20*, 184002. (c) Stepanow, S.; Lingenfelder, M.; Dmitriev, A.; Spillmann, H.; Delvigne, E.; Lin, N.; Deng, X. B.; Cai, C. Z.; Barth, J. V.; Kern, K. *Nat. Mater.* **2004**, *3*, 229–233. (d) Barth, J. V.; Weckesser, J.; Lin, N.; Dmitriev, A.; Kern, K. *Appl. Phys. A* **2003**, *76*, 645–652. (e) Ruben, M.; Rojo, J.; Romero-Salguero, F. J.; Uppadine, L. H.; Lehn, J. M. *Angew. Chem., Int. Ed.* **2004**, *43*, 3644–3662.

(2) (a) Pawin, G.; Wong, K. L.; Kim, D.; Sun, D. Z.; Bartels, L.; Hong, S.; Rahman, T. S.; Carp, R.; Marsella, M. *Angew. Chem., Int. Ed.* **2008**, *47*, 8442–8445. (b) Matena, M.; Stöhr, M.; Riehm, T.; Bjork, J.; Martens, S.; Dyer, M. S.; Persson, M.; Lobo-Checa, J.; Müller, K.; Enache, M.; Wadepohl, H.; Zegenhagen, J.; Jung, T. A.; Gade, L. H. *Chem.—Eur. J.* **2010**, *16*, 2079–2091.

(3) He, J.; Yang, C.; Xu, Z. T.; Zeller, M.; Hunter, A. D.; Lin, J. H. *J. Solid State Chem.* **2009**, *182*, 1821–1826.

(4) Che, C. M.; Li, C. H.; Chui, S. S. Y.; Roy, V. A. L.; Low, K. H. *Chem.—Eur. J.* **2008**, *14*, 2965–2975.

(5) (a) Lin, N.; Dmitriev, A.; Weckesser, J.; Barth, J. V.; Kern, K. *Angew. Chem., Int. Ed.* **2002**, *41*, 4779–4783. (b) Perry, C. C.; Haq, S.; Frederick, B. G.; Richardson, N. V. *Surf. Sci.* **1998**, *409*, 512–520. (c) Dougherty, D. B.; Maksymovych, P.; Yates, J. T. *Surf. Sci.* **2006**, *600*, 4484–4491.

(6) (a) Driver, S. M.; Woodruff, D. P. *Surf. Sci.* **2000**, *457*, 11–23. (b) Ferral, A.; Paredes-Olivera, P.; Macagno, V. A.; Patrito, E. M. *Surf. Sci.* **2003**, *525*, 85–99. (c) Keller, H.; Simak, P.; Schrepp, W.; Dembowski, J. *Thin Solid Films* **1994**, *244*, 799–805. (d) Konopka, M.; Turansky, R.; Dubecky, M.; Marx, D.; Stich, I. *J. Phys. Chem. C* **2009**, *113*, 8878–8887. (e) Maksymovych, P.; Sorescu, D. C.; Yates, J. T. *Phys. Rev. Lett.* **2006**, *97*, 146103. (f) Sardar, S. A.; Syed, J. A.; Ikenaga, E.; Yagi, S.; Sekitani, T.; Wada, S.; Taniguchi, M.; Tanaka, K. *Nucl. Instrum. Methods Phys. Res., Sect. B* **2003**, *199*, 240–243.

(7) Di Castro, V.; Bussolotti, F.; Mariani, C. *Surf. Sci.* **2005**, *598*, 218–225.

(8) Wong, K. L.; Lin, X.; Kwon, K. Y.; Pawin, G.; Rao, B. V.; Liu, A.; Bartels, L.; Stolbov, S.; Rahman, T. S. *Langmuir* **2004**, *20*, 10928–10934.

(9) Lin, N.; Payer, D.; Dmitriev, A.; Strunskus, T.; Woll, C.; Barth, J. V.; Kern, K. *Angew. Chem., Int. Ed.* **2005**, *44*, 1488–1491.

(10) Giesen, M. *Surf. Sci.* **1999**, *442*, 543–549.

(11) Giesen, M. *Prog. Surf. Sci.* **2001**, *68*, 1–153.

(12) Griessl, S.; Lackinger, M.; Edelwirth, M.; Hietschold, M.; Heckl, W. M. *Single Mol.* **2002**, *3*, 25–31.

(13) (a) Ruben, M.; Payer, D.; Landa, A.; Comisso, A.; Gattinoni, C.; Lin, N.; Collin, J. P.; Sauvage, J. P.; De Vita, A.; Kern, K. *J. Am. Chem. Soc.* **2006**, *128*, 15644–15651. (b) Otero, R.; Lukas, M.; Kelly, R. E. A.; Xu, W.; Laegsgaard, E.; Stensgaard, I.; Kantorovich, L. N.; Besenbacher, F. *Science* **2008**, *319*, 312–315. (c) Kühne, D.; Klappenberger, F.; Decker, R.; Schlickum, U.; Brune, H.; Klyatskaya, S.; Ruben, M.; Barth, J. *J. Phys. Chem. C* **2009**, *113*, 17851–17859.

(14) (a) Stöhr, M.; Wahl, M.; C.H., G.; Riehm, T.; Jung, T. A.; Gade, L. H. *Angew. Chem., Int. Ed.* **2005**, *44*, 7394–7398. (b) Stöhr, M.; Wahl, M.; Spillmann, H.; Gade, L. H.; Jung, T. A. *Small* **2007**, *3*, 1336–1340.

(15) (a) Miwa, J. A.; Cicoira, F.; Bedwani, S.; Lipton-Duffin, J.; Perepichka, D. F.; Rochefort, A.; Rosei, F. *J. Phys. Chem. C* **2008**, *112*, 10214–10221. (b) Miwa, J. A.; Cicoira, F.; Lipton-Duffin, J.; Perepichka, D. F.; Santato, C.; Rosei, F. *Nanotechnology* **2008**, *19*, 424021.

(16) Pivetta, M.; Blüm, M.-C.; Patthey, F.; Schneider, W.-D. *Angew. Chem., Int. Ed.* **2008**, *47*, 1076–1079.

(17) Blüm, M.-C.; Cavar, E.; Pivetta, M.; Patthey, F.; Schneider, W.-D. *Angew. Chem., Int. Ed.* **2005**, *44*, 5334–5337.

(18) Tomba, G.; Stengel, M.; Schneider, W.-D.; Baldereschi, A.; De Vita, A. *ACS Nano* **2010**, *4*, 7545–7551.

(19) Voznyy, O.; Dubowski, J. J.; Yates, J. T.; Maksymovych, P. *Angew. Chem., Int. Ed.* **2009**, *131*, 12989–12993.

(20) Steudel, R. *Angew. Chem., Int. Ed. Engl.* **1975**, *14*, 655–664.

(21) Ahte, P.; Palumaa, P.; Tamm, T. *J. Phys. Chem. A* **2009**, *113*, 9157–9164.

(22) Hermann, H. L.; Boche, G.; Schwerdtfeger, P. *Chem.—Eur. J.* **2001**, *7*, 5333–5342.

(23) Marschall, M.; Reichert, J.; Weber-Bargioni, A.; Seufert, K.; Auwärter, W.; Klyatskaya, S.; Zoppellaro, G.; Ruben, M.; Barth, J. V. *Nature Chem.* **2010**, *2*, 131–137.

(24) Kelly, R. E. A.; Lukas, M.; Kantorovich, L. N.; Otero, R.; Xu, W.; Mura, M.; Laegsgaard, E.; Stensgaard, I.; Besenbacher, F. *J. Chem. Phys.* **2008**, *129*, 184707.

(25) (a) Gutzler, R.; Walch, H.; Eder, G.; Kloft, S.; Heckl, W. M.; Lackinger, M. *Chem. Commun.* **2009**, 4456–4458. (b) Walch, H.; Gutzler, R.; Sirtl, T.; Eder, G.; Lackinger, M. *J. Phys. Chem. C* **2010**, *114*, 12604–12609.

(26) Zhang, J. M.; Song, X. L.; Zhang, X. J.; Xu, K. W.; Ji, V. *Surf. Sci.* **2006**, *600*, 1277–1282.